EVOLUTION OF INTERSTELLAR GAS IN RAPIDLY ROTATING ELLIPTICAL GALAXIES: FORMATION OF DISKS[1]

Fabrizio Brighenti[2,3] and William G. Mathews[3]
[2]Dipartimento di Astronomia, Università di Bologna, via Zamboni 33, Bologna 40126, Italy
brighenti@astbo3.bo.astro.it
[3]University of California Observatories/Lick Observatory, Board of Studies in Astronomy and Astrophysics, University of California, Santa Cruz, CA 95064
mathews@lick.ucsc.edu

ABSTRACT

We describe the evolution of interstellar gas in a family of low luminosity elliptical galaxies all having $M_B = -20$ but with different degrees of flattening (E0, E2, and E6) and two current supernova rates, SNu = 0.01 and 0.04. The galaxies are composed of 90 percent dark matter, are rotationally flattened and have isotropic stellar velocity dispersions.

The soft X-ray luminosity of the hot interstellar gas after evolving for 15 Gyrs decreases dramatically with increasing galactic rotation. As the rotating hot interstellar gas loses energy in the galactic potential, it cools onto a large disk. The outer radius of the disk can be much reduced by increasing the supernova rate which drives a gentle galactic wind transporting high angular momentum gas out of the galaxy. The total mass of cooled disk gas is less sensitive to the supernova rate.

Although the hot interstellar gas may be difficult to observe in rotating low-luminosity ellipticals, the cooled disk gas can be observed (i) in optical line emission since part of the cooled disk gas is photoionized by stellar UV and (ii) in the optical continuum, assuming the colder disk gas forms into luminous stars. The mass of HII gas ($\sim 10^8\ M_\odot$) may be much greater than previously realized since rotationally supported, low density HII contributes little to the global optical line emission. We interpret the stellar disks that are common (or ubiquitous) in low luminosity ellipticals as stars that have formed in the cold disk gas. The total mass of cold disk gas available for star formation is similar to the masses of stellar disks observed. The high stellar Hβ photometric index observed in disky ellipticals can be understood by combining the light of young disk stellar populations with that of the old bulge population.

Subject headings: galaxies: evolution – galaxies: disks – galaxies: interstellar gas

1. INTRODUCTION

In a previous paper we discussed the evolution and X-ray appearance of hot interstellar gas in a family of massive, slowly rotating, isolated elliptical galaxies having different ellipticities and rotation rates (Brighenti & Mathews 1996, a.k.a. Paper 1). When large, non-rotating ellipticals are flattened by anisotropic stellar velocities we found that the X-ray images are rather insensitive to variations in the galactic ellipticity. However, when a small rotation is introduced the X-ray images become significantly flatter than the optical image when viewed perpendicular to the axis of rotation. As the hot gas flows inward in the galactic "cooling flow," it forms a large disk comparable in radius to the effective radius and

spins up to the local disk-plane circular velocity which can be quite large for massive ellipticals, ~ 500 km s^{-1}, a velocity that should be resolved with AXAF. After evolving from 1 Gyr, when early galactic winds are assumed to have subsided, to 15 Gyrs, about ten percent of the total baryonic mass of the galaxy cooled into this large disk. The final disposition of this cooled gas is uncertain; low-mass star formation is one possibility but a significant amount of gas may remain as low density HII gas ionized by the stellar UV.

Now we wish to examine the evolution and X-ray appearance of interstellar gas in a second type of elliptical galaxy having a lower luminosity and larger rotation. In recent years it has become apparent that the stellar properties of elliptical galaxies divide into two types: ellipticals of high luminosity having (modestly) triaxial shapes, boxy isophotes, more pronounced central cores, less rotation and (limited) flattening by anisotropic stellar dispersion; by contrast, ellipticals of low luminosity generally have disky isophotes, dense central stellar cusps, rotationally induced flattening, approximately axisymmetric geometry and isotropic stellar velocities (Davies et al. 1983; Nieto et al. 1991; Kormendy & Bender 1996; Tremblay & Merritt 1996; Faber et al. 1997) The changeover in elliptical properties occurs over a range of luminosities, $M_V \sim -20$ to -22 where both types coexist. Both high and low luminosity ellipticals coexist on the fundamental plane (Faber et al. 1997).

Our interest in the evolution of hot interstellar gas in low luminosity ellipticals has been motivated in part by the prospect of better X-ray observations that will be provided by AXAF in the near future. In low luminosity ellipticals the X-ray emission from the hot gas is likely to be masked by the collective emission from (low-mass) X-ray binary stars (e.g. Kim, Fabbiano & Trinchieri 1992). However, the stellar X-ray component is expected to have the same surface brightness distribution as the optical image so it should be possible in principle to subtract the stellar contribution from high quality AXAF images, leaving only the emission of the hot gas. Although such a subtraction would be difficult because of the low x-ray luminosity of the gas, it would be helped by the different surface brightness distributions expected for stars and gas (see below), by consistent x-ray surface brightness fluctuations anticipated from the stellar component, and by the dissimilar x-ray spectra of stars and gas. The characteristic stellar velocity dispersion (stellar temperature) in ellipticals decreases with total stellar mass, $T_* \propto \sigma_*^2 \propto M_{*t}^{0.32}$ (Faber et al. 1997) so the temperature of thermalized interstellar gas in virial equilibrium should also decrease with galactic mass and luminosity. However, the galactic binding energy is also proportional to σ_*^2 so any additional source of energy in the interstellar gas, such as supernova explosions, may cause the interstellar gas in low luminosity ellipticals to become unbound and flow out of the galaxy as a wind. Little is known at present about the X-ray emission from rapidly rotating, coreless, disky, low luminosity ellipticals; NGC 4697 may be the only such elliptical with measured X-ray fluxes (Fabbiano, Kim, & Trinchieri 1992). While the evidence for hot gas is currently weak or nonexistent, more may be learned in the near future.

The gas-dynamical history of low luminosity, disky ellipticals is also of interest because the stellar disks may result from star formation in the disk of cold gas that is a natural product of rotating cooling flows. The sense of rotation of the stellar disks is identical to that of the bulge component, supporting an internal origin for the stellar disks rather than formation in a merging event. Recently de Jong & Davies (1997) have reported that disky ellipticals have higher Hβ photometric indices, indicating the presence of youthful stars. They suggest that stars in the disk component, if sufficiently young, could account for the apparent youthful age of the entire galaxy as determined by the population studies of Worthey (1994) and others. It is of some interest therefore to explore the possibility that star formation has occurred in the disks of cold gas that are expected in rapidly rotating ellipticals.

Finally, the large rotationally supported disks of cooled gas are exposed to ultraviolet ionizing radiation present in galactic starlight. This raises the interesting possibility that the ionized component of these disks

can be (or has been) observed in faint optical line emission. We find that surprisingly large masses ($\sim 10^9$ $M_\odot$) of warm ($T \sim 10^4$ K), low density HII gas can reside in the outer parts of these gaseous disks where is it supported by rotation at the local galactic circular velocity and in pressure equilibrium with the ambient hot interstellar gas. The density of most of this HII gas is very low and radiates line emission extremely weakly. The presence of this warm component, which has not previously been discussed, eases somewhat the mystery regarding the ultimate disposition of galactic cooling flow gas after it cools.

In the following we discuss the evolution of hot interstellar gas in a family of six low luminosity, ellipticals having different ellipticities, angular momenta and supernova heating rates. As in Paper 1 we consider the rotating galaxies to be isolated; gas inflow or ram pressure effects expected in a cluster environment are not considered here. We find that the radial extent of the disks, the mass of gas entering the disks, and the current mass of hot interstellar gas throughout the galaxies are all very sensitive to the assumed Type Ia supernova rate, assuming that the supernova energy is shared throughout the interstellar gas. In the most favorable circumstances for disk formation in rapidly rotating galaxies, the disks are very extended.

2. GALACTIC MODELS

A variety of double power law density models has been proposed for spherical elliptical galaxies (Jaffe 1983; Hernquist 1990; Dehnen 1993; Tremaine et al. 1994). Some of these provide excellent global approximations to de Vaucouleurs profiles while others (Faber et al. 1997) are designed to match central density profiles observed with HST. However, apart from their success in fitting the projected surface brightness distribution, the lack of dark matter and infinite extent of these double power law models make them inappropriate for determining stellar velocities for our models. On the other hand we find that the projected surface brightness of King profiles are adequate approximations to de Vaucouleurs profiles, certainly for our purposes here, and also have much mathematical simplicity particularly when extended to include oblate galaxies.

For these reasons we have decided to retain the models used in our previous paper (Brighenti & Mathews 1996, Paper 1) on more luminous ellipticals: simplified King profiles for the stellar density and pseudo-isothermal structures for the dark matter distribution, i.e.

$$\rho_*(m_o{}^2) = \rho_{o*}(1 + (R_t/R_{c*})^2 m_o^2)^{-3/2} \qquad \rho_h(m_o{}^2) = \rho_{oh}(1 + (R_t/R_{ch})^2 m_o^2)^{-1}.$$

The two density distributions depend on a single parameter $m_o^2 = (R/R_t)^2 + (z/z_t)^2$ and are both truncated at some large elliptical surface defined by R_t and $z_t = R_t(1-e^2)^{1/2}$ where e is the eccentricity of both the stellar and dark matter. We generate a family of equal-mass elliptical En galaxies all having the same ρ_{o*} and ρ_{oh} by scaling the $R-$core radius according to $R_{c*} = R_{c*}^{(s)}(1-0.1n)^{-1/3}$ where $R_{c*}^{(s)}$ is the core radius of the spherical galaxy. The detailed procedure used in constructing the models and the total galactic potential (both within and beyond the galactic mass distribution) are described in Paper 1. As in Paper 1 we solve the two dimensional Jeans equations to find the stellar temperature

$$T_*(R,z) = \frac{\mu M}{3k_B}(2\sigma^2 + \sigma_\phi^2)$$

at every position in the galaxy. Here $\sigma^2 = \sigma_R^2 = \sigma_z^2$ is the stellar velocity dispersion in the meridional plane and σ_ϕ^2 is the random stellar dispersion in the azimuthal direction. In Paper 1 we employed the Satoh

decomposition of the mean square azimuthal speed into a random dispersion and a systematic rotation:

$$\overline{v_\phi{}^2} = \sigma_\phi{}^2 + \overline{v_\phi}^2$$

where

$$\sigma_\phi^2 \equiv \overline{v_\phi{}^2} - \overline{v_\phi}^2 = k^2\sigma^2 + (1-k^2)\overline{v_\phi{}^2}$$

(Satoh 1980). In general $k^2(R, z)$ is an unknown function of both spatial coordinates, but is usually regarded as constant throughout the galaxy. In this current paper we consider only galaxies that are rotationally flattened, i.e. $k^2 = 1$ and which therefore must have have isotropic velocity ellipsoids. The evaluation of the potential and stellar velocity dispersion simplifies considerably in the spherical limit, see Paper 1 for further details.

We use an extended Hubble nomenclature to describe our models: EnA;k^2 where En is the normal Hubble designation with $n = 10[1-(1-e^2)^{1/2}]$, k is the Satoh parameter and A = H or L is an additional optional distinction that characterizes the "high" or "low" supernova rate assumed (as explained below). We consider here a family of galactic models all having the same luminosity, central densities, and total mass but with different degrees of rotationally induced flattening. In Table 1 we list the parameters of the spherical member of the family, E0;0. The basic parameters that define the stellar distribution, R_e, L_B and σ_* are chosen so that the galaxy lies on the fundamental plane (Tsai & Mathews 1995; Paper 1). These parameters are also nicely consistent with recent fits to HST observations (Faber et al. 1997) with one exception: our stellar core radius $R_{c*} = 63$ pc is about ten times larger than upper limits for possible cores in "power-law" galaxies of the same absolute magnitude. If we decrease the core radius to be consistent with the HST upper limits while also maintaining the Tsai-Mathews fundamental plane relationships, we find that the overall luminosity of the galaxy becomes too faint to be of much interest ($M_V \gtrsim -18$). Nevertheless, the galaxy described in Table 1 is entirely satisfactory for our models of the global large-scale evolution of interstellar gas throughout the galaxy in which the stellar core region has no influence and is poorly resolved by the hydrodynamic grid. Finally we note that the central density and core radius of the dark matter component have been chosen so that the total dark mass is 9 times that in the stellar component and its distribution is such that dark matter has little influence on stellar velocities within ~ 1 effective radius.

Figure 1 shows the distribution of stellar temperature $T_*(R, z)$ and azimuthal velocity $v_{*\phi}(R, z)$ in a quadrant of the E2;1 member of the galactic family corresponding to the E0;0 galaxy in Table 1. At the outer edge of the galaxy the stellar velocity dispersions in the meridional plane must vanish since no stars can move beyond this surface; however, when $k = 1$ the dispersion is isotropic and the azimuthal dispersion σ_ϕ^2 (and T_*) must also vanish at the outer galactic boundary. Consequently, the contours of $T_*(R, z)$ are much more elliptical than those of the (slowly rotating) E2;0.25 galaxy shown in Paper 1.

The azimuthal stellar velocity $v_{*\phi}(R, 0)$ and circular velocity on the equatorial plane are illustrated in Figure 2. The rather strong maximum in $v_{*\phi}(R, 0)$ at a few hundred parsecs from the galactic center, particularly for the E6;1 galaxy, may differ from stellar rotation curves observed in some low luminosity ellipticals [e.g. NGC 4697 observed by Binney, Davies, and Illingworth (1990)], but stellar rotation curves are unavailable for most of the low luminosity ellipticals known to have power-law density profiles. In any case, the global interstellar gas dynamics are not strongly influenced by this maximum in $v_{*\phi}(R, 0)$. As the hot interstellar gas cools and flows inward, it is expected to spin up to the local circular velocity $v_{circ}(R)$ and become rotationally supported.

3. GAS DYNAMICS

The gas dynamical equations are identical to those used in Paper 1. Interstellar gas is created by normal mass loss from an evolving population of old stars at a rate

$$\alpha_*(t)\rho_* = \alpha(t_n)(t/t_n)^{-1.3}\rho_* \quad \text{gm cm}^{-3}\ \text{s}^{-1}$$

where $t_n = 15$ Gyr represents the present time and $\alpha(t_n) = 5.4 \times 10^{-20}$ s^{-1} (Mathews 1989). The contribution of gas from Type Ia supernovae to the interstellar mass is negligible ($\alpha_{sn} \ll \alpha_*$) but is more energetic and iron-rich. The energy generated at early times by Type II supernovae is expected to expel most of the interstellar gas created prior to some time which we adopt as 1 Gyr. Between 1 and 15 Gyrs about one tenth of the stellar mass remaining at $t = 1$ Gyr enters the interstellar medium. For simplicity, we do not vary the galactic potential during this time interval to account for this small stellar mass loss.

The temperature of the interstellar gas is similar to the local stellar temperature since both components are in hydrostatic equilibrium in the galactic potential, although the gas can also be heated by supernova explosions. The characteristic source-term temperature for the gas is

$$T_o = (\alpha_* T_* + \alpha_{sn} T_{sn})/\alpha_*$$

where $\alpha_{sn} \ll \alpha_*$ is assumed. Heating by supernova explosions is given by

$$\alpha_{sn} T_{sn} = 2.13 \times 10^{-8}\ \text{SNu}(t)\ (E_{sn}/10^{51}\text{ergs})\ h^{-1.7}\ (L_B/L_{B\odot})^{-0.35} \quad \text{K s}^{-1}$$

(see Mathews 1996) where $h \equiv H/100 = 0.75$ is the reduced Hubble constant and we adopt $E_{sn} = 10^{51}$ ergs as the typical hydrodynamic energy released in a supernova event. The temperature $T_{sn} = m_p E_{sn}/3km_{sn}$ (m_p = proton mass) depends on the average mass lost per supernova m_{sn}. The total rate that supernovae supply gas to a galaxy of mass M_{*t} is $\alpha_{sn} M_{*t} = \nu_{sn} m_{sn}$ where ν_{sn} is the supernova rate in sec^{-1}; to convert ν_{sn} to SNu units (number of supernovae per 100 years from stars of luminosity $L_B = 10^{10} L_{B\odot}$) we use the mass to light ratio determined by van der Marel (1991), $M_{*t}/L_B = 2.98 \times 10^{-3} L_B^{0.35} h^{1.7}$ where L_B is in $L_{B\odot}$. The supernova rate is assumed to decrease with time as a power law:

$$\text{SNu}(t) = \text{SNu}(t_n)(t/t_n)^{-1},$$

although there is at present no compelling observational reason to adopt this form. We consider two values for the current supernova rate, SNu$(t_n) = 0.01$ and SNu$(t_n) = 0.04$. These rates are comparable with the most recent observed value SNu$_{obs}(t_n) = 0.12 \pm .06\ (h/0.75)^2$ (Turatto, Cappellaro & Benetti 1994). We do not expect exact agreement between the observed value SNu$_{obs}(t_n)$ and the factor SNu(t_n) in the expression above for $\alpha_{sn} T_{sn}$ since SNu(t) is only one of several uncertain parameters that influence $\alpha_{sn} T_{sn}$ in our gas dynamical models. With the higher value of SNu we find that the iron abundance in the interstellar gas exceeds those observed by the ASCA satellite; possible origins of this discrepancy have been discussed by Arimoto et al. (1997). For simplicity we distribute the supernova energy (and iron!) smoothly throughout the interstellar gas; the accuracy of this often-used assumption is difficult to access since the initial deposition of supernova energy is localized in hot interstellar bubbles (Mathews 1990). Since $\alpha_*(t)$ decreases with time more rapidly than SNu(t), the influence of supernova heating (and the likelihood of galactic winds) increases with time in our models.

As in Paper 1 we assume that the galaxy is completely isolated, allowing hot gas to flow freely beyond the stellar edge. The gas flow is regarded as invicid, i.e. the magnetic field is sufficiently large to drastically

reduce the plasma mean free path yet the field is sufficiently disordered on small scales ($\ll R_e$) not to communicate stresses over large distances in the interstellar gas. For numerical solutions describing the evolution of the interstellar gas we used the NCSA Eulerian hydrocode ZEUS2D, appropriately modified as described in Paper 1.

4. COOLING FLOW EVOLUTION

4.1. The Spherical E0;0 Galaxy

The influence of galactic rotation on the nature and evolution of interstellar gas in ellipticals can be determined by comparison with otherwise identical spherical, non-rotating models. Properties of the interstellar gas in the non-rotating E0;0 galaxy at time $t_n = 15$ Gyr are shown in Figure 3. The interstellar gas flows in a axisymmetric cylindrical computational grid of 120 × 120 zones with gradually increasing zone size; the smallest central zone is half the stellar core radius. Solutions are initiated at time $t = 1$ Gyr, when it is assumed that SNII explosions and early galactic winds have subsided, and continued to 15 Gyrs with two values of the current supernova rate, SNu(t_n) = 0.01 (E0L;0) and SNu(t_n) = 0.04 (E0H;0). The linear excursions of the gas density and temperature at small radii in Figures 3a and 3b are artifacts of the limited spatial resolution in the innermost grid points. The temperature of the gas is slightly larger than the virial temperature for the solution with the higher supernova rate (E0H;0) so some gas flows out of the galaxy. As a result the gas density and X-ray surface brightness in the E0H;0 galaxy are lower than for the E0L;0 galaxy while the gas temperature in the E0H;0 galaxy is higher, particularly in the outer parts of the galaxy. The X-ray surface brightness is calculated for the 0.1 - 2.4 keV energy band to approximate ROSAT observations.

The effect of changing the supernova rate is also apparent in Table 2 which lists several global properties of these models. The mass of hot gas within the galactic boundary $M_g(hot)$ and (especially) the total soft X-ray luminosity L_x (0.1 - 2.4 keV) are both reduced when the supernova rate is increased. The total amount of cold gas that accumulates in the galactic core $M_g(cold)$ is also significantly lower as a result of gas outflow.

The gas velocity in these spherical galaxies is very subsonic everywhere. As gas loses energy by radiation it sinks subsonically in the galactic potential and is maintained at approximately constant temperature by Pdv compression in the galactic potential. Superimposed on this global flow are low-amplitude, highly subsonic random motions ($\sim 10 - 20$ km s^{-1}). We believe these random velocities are numerical in origin, but similar small velocities could be generated in real galaxies by small physical irregularities. These small velocities are nevertheless sufficient to prevent the appearance of a "galactic drip" or global thermal instability (Mathews 1997) that appears when these same calculations are performed with a 1D spherically symmetric grid. The implications of these results for the reality of galactic drips are unclear at present.

4.2. Cooling Flow Evolution in E2;1 and E6;1 Galaxies

4.2.1. Formation of Cold Disks

As expected from angular momentum conservation, in rotating galaxies the gas cools into a large, rotationally supported disks . Gas that cools below 10^4 K is held at this temperature throughout the remainder of the calculation. The mass of this cold gas in the disk generally increases with time. The total vertical column density in cooled gas is shown at three times in Figures 4a, b, and c for the disks of the E2L;1, E2H;1, and E6L;1 galaxies respectively. The E2H;1 elliptical with the higher supernova rate (Fig. 4b) has a much less extended disk owing to the outflow of (high angular momentum) gas from the galaxy in a slow wind. At the last time plotted in Figure 4b the E2H;1 disk has actually become smaller probably as a result of local heating of gas by supernovae. However, the large disks that form in the E2L;1 and E6L;1 galaxies are very similar. In both disks the outer edge increases with time, similar to the growth pattern of disks in more slowly rotating ellipticals (Paper 1) and the surface density increases slowly within the body of the disk, indicating that gas enters the disk at all radii, not just at the outer edge. The similarity of Figures 4a and 4c indicates that the column density beyond several stellar core radii is almost independent of the degree of galactic rotational flattening. The E2L;1 and E6L;1 galaxies both have power-law, not exponential, disks with surface densities given by $\Sigma_d \propto R^{-1.93}$.

Even in these maximally rotating galaxies with $k^2 = 1$, gas ejected from stars moves a considerable distance from its point of origin toward the rotation axis before settling into the cold disk. As gas moves along a streamline toward the disk, it mixes with locally produced gas having different angular momentum. In spite of this complication, it is possible to estimate the radius $R_d(R, z)$ in the disk where mass lost from stars at R, z will eventually cool (see Paper 1). In Figure 5 we plot contours of equal $R_d(R, z)$ for the E2:1 galaxy. These contours are (implicit) solutions of $R_d v_{circ}(R_d) = R v_{*\phi}(R, z)$, the condition that an element of gas ejected by stars at R, z strictly preserves its specific angular momentum until it reaches the disk at radius R_d. For example, Figure 5 indicates that gas ejected from stars at $R \sim 20$, $z \sim 20$ kpc has the same angular momentum as gas in the disk at $R_d \approx 4$ kpc.

4.2.2. Nature of Interstellar Medium at $t_n = 15$ Gyr

The flow in galaxy E2L;1 shown in Figure 6 exhibits subsonic kinetic activity and corresponding irregularities in the density contours, particularly in the outer galaxy. Within about 10 kpc, however, the flow toward the central disk is regular and the density contours have an ellipticity similar to that of the local stars. However, notice that a relatively dense and cold region has appeared in the flow at time $t_n = 15$ Gyr near $R = 40$, $z = 3$ kpc. This cold, transient lump of gas is falling toward the disk plane where it will eventually reside. Such intermittent contributions to the far outer edge of the cold disk are also evident from Figure 4 and may be a generic feature in rapidly rotating cooling flows. Similar inhomogeneities have also appeared in the calculations of D'Ercole & Ciotti (1997) who are studying the evolution of hot gas in S0 galaxies. At time $t = 15$ Gyrs the most rapid rotation above the disk plane, $v_\phi \sim 220$ km s^{-1}, is near $R \approx 28$ kpc; the full width of emission line profiles in the X-ray spectrum of this galaxy is ~ 440 km s^{-1}, within the resolution capability of AXAF.

The irregular velocity field in Figure 6, unlike the laminar flow in the slowly rotating galaxies described in Paper 1, may result from shear instabilities that first develop in the low density outer galaxy. The azimuthal velocity of gas just within the galaxy is driven somewhat by ejecta from azimuthally streaming stars. Such an interaction may enhance shear instabilities at the galactic boundary, but we have not investigated in detail the physical origin of these very subsonic velocities.

When the supernova rate is increased by a factor of 4, a subsonic wind develops throughout most of the galaxy at time $t_n = 15$ Gyr as shown in Figure 7. The gas density is lower and its spatial variation is more regular in this gentle galactic wind than in the flow in Figure 6. Since we assume that mass enters the flow at a rate $\alpha_* \propto t^{-1.3}$ that decreases faster than the supernova rate, SNu(t) $\propto t^{-1}$, the thermal energy delivered to each gram of interstellar gas slowly increases with time and the overall solution tends toward a galactic wind as the calculation proceeds. Finally, in Figure 8 we show the density and velocity fields at $t_n = 15$ Gyr in the rapidly rotating E6L;1 galaxy. In such flat galaxies incipient winds first appear near the outer edge of the equatorial plane near $R \sim 80$ kpc. Winds occur first in the equatorial region because (i) the (more spherical) gravitational potential is less here and (ii) the presence of rotation reduces the effective potential. Notice that there is another "lump" of cooling gas descending toward the equatorial plane at $R \approx 45$ kpc similar to the cool lump discussed in Figure 6.

4.2.3. Soft X-ray Images

The appearance of the hot interstellar gas when viewed in soft X-rays (0.1 - 2.4 keV) is shown for three galaxies in Figure 9. The galactic breeze driven by supernova heating in the E2H;1 galaxy has a dramatic effect in circularizing the X-ray image compared to that of the E2L;1 galaxy of the same age. However, it is unclear if the emission from the hot gas illustrated in Figure 9 can be observed because it is masked by the collective emission from low mass X-ray binaries in the stellar component. Ideally, with high signal to noise AXAF observations it would be possible to subtract the soft X-ray contribution from stars since the stellar surface brightness distribution is known from optical observations. Although the possibility of such a decomposition to find the X-ray emission from the gas alone was one of the initial motivations for our series of calculations, the X-ray luminosities of the interstellar gas in the rotating galaxies in Table 2 may be too small to be detectable. The stellar L_x from ellipticals is poorly known, but Ciotti et al. (1991) suggest $L_{x,*} \approx 1.5 \times 10^{40}(L_B/10^{11})$ ergs s^{-1} which for our galaxy is $L_{x,*} \approx 2 \times 10^{39}$ so the L_x from the interstellar gas will be a disky component only a few percent of the total – a challenging observation even for AXAF. The X-ray emission from non-rotating galaxies in Table 2 could be observed quite easily, but it is unlikely that many low luminosity galaxies are either spherical or non-rotating (Tremblay & Merritt 1996).

5. PHYSICAL NATURE OF THE COOLED GAS

The final physical configuration of cooled gas in galactic and cluster cooling flows remains one of the most perplexing unsolved problems in galactic evolution. The usual solution is to assume that stars of very low mass and luminosity form in these high-pressure environments; there is currently no strong observational evidence against this hypothesis. In the following discussion, however, we examine two new aspects of this problem that arise when galactic rotation is considered. First, regardless of the final endstate of the cooled gas, there will always be some disk gas that cannot form into stars because it is photoionized by the galactic and intergalactic ionizing radiation fields. We discuss below the mass and possible observability of this ionized gas. Second, we consider the hypothesis that relatively young luminous stars have formed in the cooled gaseous disks and that these disk stars are responsible for the systematically larger Hβ photometric indices observed in disky ellipticals of low luminosity.

5.1. Emission from HII gas at $T \approx 10^4$ K

Some of the gas that cools onto the rotating disk is kept ionized by ambient ionizing radiation and remains at $T \approx 10^4$ K, the same temperature we have adopted for all the cooled gas. In the inner parts of our disks the maximum column depth of HII gas that can be ionized by the available radiation, N_i, is much less than the total column of cooled disk gas N_{tot}. Such a layer of ionized gas should be stable toward forming gravitational irregularities. However, regions deeper in the disk than N_i are in reality expected to be colder than $T = 10^4$ K and are probably unstable to cloud (and star?) formation. If dense condensations should form in this colder gas, the HII gas should still be present as a distributed component having a column density $\sim N_i$. In the inner disk therefore we expect a column N_i of HII gas to always be present even if most of the colder disk gas is highly clumped or stellar. In addition, our solutions indicate that a considerable mass of HII gas may be present in the outer disk provided the supernova rate is low. Figure 10 shows a plot of the variation of the total column of cold gas N_{tot} and the maximum amount that can be ionized N_i. Beyond about $R \sim 9$ kpc in the E2L;1 galaxy all the disk is fully ionized. We describe below how we have estimated the column N_i and the total mass of HII gas. We also discuss the likelihood of detectable optical line emission from the HII disk. The ionizing radiation has both galactic and extra-galactic components.

Stellar UV flux has been measured in seven ellipticals from 1800 Å to the Lyman edge (Ferguson & Davidsen 1993; Brown, Ferguson, & Davidsen 1995) and Binette et al. (1994) have estimated the entire UV spectral energy distribution and the total galactic ionizing photon luminosity $\mathcal{L}_t$ from the collective radiation of post-AGB stars in an old stellar population. Such estimates are very uncertain since the evolutionary tracks of highly evolved stars and their atmospheres are poorly understood. At time $t = 13$ Gyr following a single burst of star formation, Binette et al. find $\mathcal{L}_t \approx 7.3 \times 10^{40}$ s^{-1} $M_{\odot}{}^{-1}$; for our galaxy this is $\mathcal{L}_t \approx 5.5 \times 10^{51}$ s^{-1}. We have attempted to reconcile this estimate with the UV observations by averaging values of $\nu L_\nu/(L_B/L_{B,\odot})$ at 1100 Å and 1500 Å for the six galaxies observed by Brown, Ferguson, & Davidsen (1995). Our values of L_B are based on $h = 0.75$ and the galactic properties listed by Faber et al. (1997). Individual values of $\nu L_\nu/(L_B/L_{B,\odot})$ at both wavelengths range over a factor of about four, but the ratio of the mean values at these two wavelengths agrees almost exactly with the slope of the UV spectral energy distribution in this part of the spectrum given in arbitrary units by Binette et al. (1994). Using the UV observations at these two wavelengths to calibrate the ionizing continuum of Binette et al. (1994) we find $\mathcal{L}_t \approx 2.0 \times 10^{41}(L_B/L_{B,\odot})$ s^{-1} which for our galaxy (e.g. Table 1) is $\mathcal{L}_t \approx 2.6 \times 10^{51}$ s^{-1} in good agreement with the estimate of of Binnette et al. We shall therefore adopt here a value $\mathcal{L}_t = 5 \times 10^{51}$ s^{-1} at $t = 15$ Gyr which is slightly less than the value from Binnette et al. at $t = 13$ Gyr since $\mathcal{L}_t$ slowly decreases with time. Some of this Lyman continuum radiation is consumed ionizing dense circumstellar gas in newly formed planetary nebulae, but we expect this fraction to be small since the nebular gas is swept back along the stellar orbit by ram pressure on time scales short compared to the total UV lifetime of the central stars (Mathews 1990). If the total stellar ionizing photon emissivity follows the starlight, $j_{iph} = j_o[1 + (R/R_{c*})^2]^{-3/2}$, we determine the coefficient $j_o = 2.4 \times 10^{-12}$ cm^{-3} s^{-1} and the ionizing photon density at any radius in the galaxy by using the expressions for the radiation density from Tsai and Mathews (1995). For simplicity we use the spherical relations of Tsai and Mathews to estimate the stellar ionizing photon density and ionized column in the disk of the moderately flattened E2L;1 galaxy. For the intergalactic contribution to the ionizing photon density we use the value $n_{iph,ig} \approx 4 \pm 2.5 \times 10^{-6}$ cm^{-3} (Dove & Shull 1994) which is constant throughout the galaxy.

The ionized column along the disk plane $N_{HII} = \min(N_i, N_{tot})$ is shown in Figure 10 for the E2L;1 galaxy at time $t = 15$ Gyrs. Beyond the galactic core radius in the E2L;1 galaxy the ionizing photon density

varies as $n_{iph} \approx 3 \times 10^{-3} R_{kpc}^{-1.5}$ cm^{-3}. This stellar ionizing UV dominates the intergalactic component throughout most of the galactic volume within ~ 35 kpc which includes all of the disk region. We assume that the HII gas in the disk is in pressure equilibrium with the local hot interstellar gas and has temperature $T \approx 10^4$ K everywhere. Since the temperature of the cooled gas in our computations is constrained to $T = 10^4$, it already has the appropriate density for the HII gas although the density in our cold isothermal disks decreases somewhat away from the disk midplane. Beyond the galactic core radius R_{c*} along the midplane of the disk the density of HII gas decreases sharply with radius: $n_i \approx 50 R_{kpc}^{-3.0}$ cm^{-3}. Estimates of the total mass of HII gas in ellipticals based on a single assumed density are therefore misleading and incorrect. In the dense inner parts of the disk only a small fraction of the cold disk gas can be ionized but beyond about 9 kpc all the disk gas is ionized. The total mass of ionized gas is very large, 8×10^8 $M_\odot$, more than ten percent of the total amount of gas that cooled in the disk since 1 Gyr (Table 2). The mass of HII gas within radius R along the disk $M_i(< R) \approx 8.7 \times 10^5 R_{kpc}^{2.62}$ $M_\odot$ (valid from $R_{kpc} = 1$ to 12.6) increases dramatically toward the outer parts of the disk where most of the HII mass resides. The total column density of all the gas that has cooled after $t = 15$ Gyr is large, $N_{tot} \approx 5.8 \times 10^{-21}$ $R_{kpc}^{-2.25}$ cm^{-2} (valid from $R_{kpc} = 0.1$ to 10). This gas cannot be smoothly distributed in the disk (i.e. not in form of clouds or stars) since it would be easily observed by X-ray absorption out to 2.5 kpc where $N_{tot} \sim 10^{21}$ cm^{-2}. However, when self-gravity of the HII gas is included we find that it is gravitationally stable against collapse at every radius in the disk so the HII gas will not form into clouds.

The total Hβ luminosity from the disk in our E2L;1 galaxy, $L_{H\beta} \approx 8 \times 10^{39}$ ergs s^{-1}, corresponds to a flux $F_{H\beta,20} \approx 1.6 \times 10^{-13}$ ergs cm^{-2} s^{-1} when viewed at a distance of 20 Mpc. This luminosity and flux are comparable to those observed in ellipticals of similar optical brightness (e.g. Trinchieri & di Serego Alighieri 1991) so we can expect that ionized disks contribute a substantial fraction of the total line emission from early type galaxies. Because of the strong variation of HII gas density and ionizing photon density with galactic radius, only about 4 percent of the total mass of HII in the dense central regions, $R \lesssim 3.2$ kpc, contributes half of the total Hβ luminosity while half of the total HII mass lies far out in the galaxy beyond ~ 9.3 kpc where all the disk gas is ionized. This low density HII gas at $\gtrsim 9$ kpc emits only ~ 10 percent of the total $L_{H\beta}$ over a vast surface area and may be undetectable with present technology. However, the total Balmer line luminosity $L_{H\beta} \approx 8 \times 10^{39}$ ergs s^{-1} far exceeds the minimum luminosity expected in galactic cooling flows due to the recombination of gas cooling for the first time; for the E2L;1 galaxy this latter value is $L_{H\beta,min} \approx 3 \times 10^{36}$ ergs s^{-1} at time $t_n = 15$ Gyr. Finally we note that $L_{H\beta}$ is about 45 times larger than the soft X-ray luminosity L_x from the E2L;1 galaxy listed in Table 2 and therefore represents a significantly larger fraction of the overall galactic radiation budget.

We have examined in a similar manner the HII mass and line luminosity in the other galaxies listed in Table 2. The radial size of the disk in the E2H;1 galaxy, $R \approx 0.5$ kpc, is greatly reduced by the higher supernova heating rate assumed. The total mass of HII gas expected from the available ionizing photons is much smaller, $M_i \approx 1.6 \times 10^4$ $M_\odot$, but $L_{H\beta} \approx 1.3 \times 10^{39}$ erg s^{-1} is only six times less than that of the E2L;1 galaxy since most of the Hβ emission is from dense gas in the inner disk. The corresponding flux at 20 Mpc is $F_{H\beta,20} \approx 2.7 \times 10^{-14}$ ergs cm^{-2} s^{-1}. The relative insensitivity of the Hβ luminosity to the physical size of the disk is interesting because it cannot explain the enormous range in $L_{H\beta}/L_B$ observed; for example Trinchieri & di Serego Alighieri (1991) find that $L_{H\alpha}/L_B$ varies over a factor of 300 among ellipticals having $L_B \sim 3 \times 10^{10}$ $L_{B\odot}$. The explanation for this large spread in Balmer luminosities could lie in varying magnetic field strengths in the galactic centers; a field of $H \gtrsim 10^{-3}$ gauss in the dense HII gas near the center of our E2L;1 galaxy could sharply reduce the gas density and the Hβ emissivity. The E6L;1 galaxy has an extended disk with the following properties: $M_i \approx 1.8 \times 10^9$ $M_\odot$, $L_{H\beta} \approx 9 \times 10^{39}$ erg s^{-1}, and $F_{H\beta,20} \approx 2 \times 10^{-13}$ ergs cm^{-2} s^{-1}.

What evidence exists for the presence of HII disks in ellipticals? Smooth, extended images of ellipticals in optical emission lines (e. g. Trinchieri & di Serego Alighieri 1991; Macchetto et al 1996) do not necessarily require emission from ionized disks and indeed some HII emission from young planetary nebulae and other ionized stellar ejecta is expected throughout the galactic volume (Mathews 1990). Unfortunately it is difficult to estimate the precise amount of HII gas that has been recently ejected from stars but has not yet entered the hot phase since the rate of this transition depends on the influence of the magnetic field configuration on thermal conductivity. Buson et al. (1994) present optical line images of a sample of ellipticals known to be unusually bright in optical emission lines. These ellipticals also have LINER spectra perhaps suggesting an additional non-stellar ionization source although the line emission symmetry does not have the biconical pattern often observed in Seyfert galaxies. Buson et al. typically find smooth Hα + [NII] images within $\sim 0.3 R_e$ that are extended along the major axis (NGC 1395, NGC 1453, NGC 2974, IC 1459). The kinematics of the HII in these ellipticals indicates regular, organized rotation around the galactic center (Zeilinger et al. 1996); this rotation is consistent with disk emission but some (smaller) rotation would also be present in line emission from recent stellar ejecta distributed throughout the galactic cooling flow. In general the emission line surface density in the HII “disks” observed by Buson et al. is confined to the central regions and drops faster with radius than the stellar light. In a few ellipticals Buson et al. find that the major axis of the HII gas is misaligned with the optical axis of the stellar image (NGC 3962) or is counter-rotating (NGC 6868, NGC 7097); in these galaxies the HII disks are evidently disturbed or created possibly as a result of a recent merger event.

Several straightforward observations would help clarify the contributions of disks to the HII emission from ellipticals. The disk component is expected to have a higher ellipticity than the stellar image and this difference should be most pronounced in ellipticals having high diskyness or V/σ that are as a class viewed more nearly perpendicular to the axis of rotation. In low luminosity ellipticals of high V/σ the HII rotation velocity should be representative of the circular velocity on the disk plane which is always greater than the rotation of the bulk of the galactic stars.

5.2. Hβ Index: Evidence of Young Disk Stars

The Hβ index is one of the many observable characteristics that distinguish elliptical galaxies of high and low luminosity. This photometric index measures the strength of Balmer line absorption in the galactic spectrum and is the principal observational means of breaking the “age-metallicity degeneracy” to reveal the presence of a subpopulation of youthful stars (Gonzalez 1993; Worthey 1994; Faber et al 1995; Worthey et al. 1995). Recently de Jong & Davies (1997) have shown that Hβ is systematically larger in (low-luminosity) disky ellipticals (Kormendy & Bender 1996); they also conjectured that the young stellar subpopulation may be the stars in the disk. Using Guy Worthey’s stellar population models, de Jong & Davies combined the Hβ indices from a young (2 Gyr) stellar disk containing about 10 percent of the total galactic stellar mass with a much older component (12 Gyr) representing the bulk of the old stellar population in the galaxy. They found that the combined Hβ index of the disk and bulge is similar to the higher Hβ indices observed within $R_e/2$ in disky ellipticals.

We have described here how cold gas gradually collects in a rotationally supported disk during the slow evolution of the galactic interstellar medium. This disk provides an ideal environment to form a younger population of disk stars. Often in theoretical studies of cooling flows it is assumed that only stars of very low mass form in the cooled gas expelled from the older generation of galactic stars. We shall assume

instead that luminous, moderately massive stars form in the cold disk gas but the stellar masses in the young disk population must not extend above about 8 $M_\odot$ since no Type II supernova have been observed in ellipticals. To test this possibility more quantitatively, we have computed stellar Hβ indices assuming that the disk consists of a number of discrete population bursts having mass $\Delta M_i(t_i)$ and age t_i. These quantized bursts are listed in Table 3 for the E2L;1 and E2H;1 galactic models. The burst masses and that of the main galactic bulge are all evaluated within $R_e/2$ for comparison with the observed values of de Jong & Davies (1997). For simplicity we assume all stellar populations have solar abundance.

After creating a variety of stellar population models using Guy Worthey's website (http://www.astro.lsa.umich,edu/users/worthey/), it became clear that the Hβ index is rather insensitive to the slope or precise mass cutoffs of the IMF but does depend strongly on the ages of the youngest stars considered. Stars younger than the youngest stellar population available at the Worthey website (1 Gyr) can contribute significantly to the overall Hβ. In view of this, Guy Worthey has generously provided us with a version of his program based on Padova evolution tracks that allows stellar populations as young as 0.4 Gyr. For the same stellar population, Hβ indices based on Padova evolution tracks are ~ 0.1 lower than the evolutionary tracks used at the website. The IMF we use here has a Salpeter slope and is terminated at mass limits $m_{high} = 10$ and $m_{low} = 0.1$ $M_\odot$. For the population ages we consider (Table 3), stars near the high mass limit do not contribute to the Hβ index, they are only relevant to estimate the remnant mass. Our remnant masses are based on evolution tracks currently available at the Worthey website program.

In Table 4 we list the Hβ index of the main galactic bulge, the disk component and the two populations combined all evaluated within $R_e/2$. The Hβ indices are slightly overestimated since we have only considered the stars within a physical radius of $R_e/2$, not what would be observed in projection at this radius through the entire galaxy. On the other hand the indices are underestimated since we (i) have not considered the contribution from stars younger than 0.4 Gyr and (ii) assume that there is no time delay between the appearance of cold gas in the disk and star formation. In any case, the total Hβ indices listed in Table 4 for galaxy plus disk in the E2L;1 and E2H;1 models nicely span the range of observed values given by de Jong & Davies, H$\beta \approx 1.7 - 2.1$. This greatly supports the hypothesis that the disk stars are simply a natural outcome of cooling flow evolution. There is also some observational evidence that the disks have higher Hβ indices than the rest of the elliptical (Scorza & Bender 1996), but this needs further confirmation.

Our disks are expected to have power-law, not exponential space density and surface brightness profiles. The surface brightness distribution observed in stellar disks of very flattened disky ellipticals (E4 - E6) deviates from exponential toward power law distributions (Scorza & Bender 1995). In disky ellipticals the angular momenta of bulge and disk are always parallel (Scorza & Bender 1995; 1996); this is consistent with star formation in cooling flow disks and rules out a disk origin from random mergers. Finally, we note that our disks are formed in ellipticals that are completely supported by rotation with fully isotropic stellar velocities ($k^2 = 1$). If some anisotropy were included ($k^2 < 1$), the resulting disks would be less extended with more steeply varying surface brightness in the resulting stars.

6. DISCUSSION AND CONCLUSIONS

Hot interstellar gas in low-luminosity ellipticals is more vulnerable to outflow than that in brighter ellipticals because the specific gravitational binding energy decreases with galactic luminosity along the fundamental plane. Low-luminosity ellipticals are also thought to be rotationally flattened which causes the

X-ray luminosity of interstellar gas to decrease sharply with increasing ellipticity. In our family of galaxies all with luminosity $L_B = 1.3 \times 10^{10}$ $L_{B,\odot}$ we find that L_x is also very sensitive to the assumed supernova rate. In ellipticals having a "low" current supernova rate, SNu$(t_n) = 0.01$, $L_x(t_n)$ varies along the sequence E0; E2; E6 in the ratios 1.0; 0.0091; 0.0027. For a higher supernova rate, SNu$(t_n) = 0.04$, the corresponding ratios are: 1.0; 0.025; 0.0033. While the X-ray emission from hot interstellar gas in the E0 galaxies would be easily observed with AXAF (by subtracting the stellar component if that were possible), the prospects for observing the interstellar contribution to L_x for more realistic rotating galaxies of this L_B are less optimistic. Furthermore, low luminosity E0 galaxies are rare or non existent (Tremblay & Merritt 1996).

The influence of past and current supernova rates on L_x and other important observational parameters is not entirely clear. The higher of the two current supernova rates we consider, SNu$(t_n) = 0.04$, generates an iron abundance within the half-light radius that is 1.5 to 3 times the stellar iron abundance. Of course any observation of the X-ray iron features in rotating, low-luminosity ellipticals is likely to be representative of stellar X-ray sources, not the gas. But in more massive ellipticals the iron abundance in the interstellar gas is often much *less* than that in the stars (Arimoto et al. 1997). This could imply that the supernova iron – and possibly also its energy – is not distributed throughout the interstellar medium as we have assumed here; indeed the supernova energy is concentrated in hot bubbles that may rise in the cooling flow atmosphere. Because of this as yet unsolved problem, we cannot be sure that we have treated the supernova energy correctly in our models, particularly for the high supernova rate solutions. If our treatment of supernova energy is correct, however, the disks of cool gas are severely truncated when SNu$(t_n) \gtrsim 0.04$ due to an enhanced outflow of high angular momentum gas from the outer parts of the galaxy. The mass of the disk remaining at time $t_n = 15$ Gyr $M_g(cold)$ is reduced by ~ 1.7 as SNu(t_n) increases from 0.01 to 0.04. More luminous ellipticals such as those we discussed in Paper 1 require much higher SNu(t_n) to alter the cold disks.

Of particular interest is the possibility of observing disks of cold gas that are expected in rotating ellipticals either directly as optical line emission or indirectly in the form of a younger stellar population. The column of unionized disk gas in our disks would produce profound and observable absorption of soft X-rays, but this can be avoided since gravitational clumping is expected in this neutral or molecular gas. We have estimated the density of ionizing photons along the disk plane and computed the column density of warm HII disk gas. The presence of HII disk gas should be independent of the likelihood of star formation in the colder neutral gas. For our low value of SNu(t_n), we find that large masses of HII gas can be rotationally supported beyond ~ 9 kpc – amounting to about one tenth of all the gas ejected from galactic stars – but the density of this gas is too low to contribute to the observed optical line flux. In previous estimates of the total HII mass in ellipticals a constant HII density is usually assumed; these masses may seriously underestimate the true mass by several orders of magnitude. In the future we intend to investigate the survivability of gas in the outer disk if the galaxy is moving through an external (inter-cluster) medium. Most of the optical line emission in the disk comes from the central parts of the disk which are less sensitive to rotation and the supernova rate. The total Hβ luminosities expected from disk HII are similar to those observed in ellipticals, implying that a significant component of optical line emission from these galaxies may originate in cooling flow disks. If the disk HII emission is not masked by other sources of warm gas, the optical line-emitting gas should be (i) systematically flatter than the stellar image and (ii) rotating at the circular velocity which exceeds the local mean line of sight velocity of galactic stars.

We have found considerable support for the notion that stellar disks in low luminosity ellipticals are a natural result of the evolution of the interstellar gas. The inevitability of cold disk formation in galactic cooling flows is consistent with the finding that all low luminosity ellipticals may contain stellar disks since

many are hidden due to low inclinations (Rix & White 1990). The stellar disk and bulge are observed to share the same sense of rotation; this argues against random merging events and supports star formation in cold disks as we propose here. The total mass of gas that enters the cold disk in 1 - 15 Gyrs, about 10 percent of the total stellar mass M_{*t}, is very similar to the typical stellar mass observed in elliptical disks. Within the approximation of our galactic models (e.g. King and isothermal density profiles; constant Satoh k^2 factor, etc.) and that of current observations of stellar disks (most of which have been studied only in very flat E5 or E6 ellipticals), we believe that our non-exponential disks are similar to those observed. Only three of the nine stellar disks studied by Scorza & Bender (1995) could be modeled with exponential disks and exponential fits can always be made over a limited range in radius. Finally, we have demonstrated that the range of observed Hβ photometric indices observed in disky ellipticals is just spanned by our models if luminous stars form in the cold gaseous disks. We are implicitly assuming here that the Type Ia supernova rate may vary among ellipticals to generate a range of disk masses; at present there is no compelling reason to believe otherwise. A similar variation of disk masses could be obtained by beginning our calculation shortly before or after 1 Gyr.

If our ideas about star formation in disky ellipticals are correct, these galaxies could become ideal laboratories for studying successive generations of star formation. In principle abundances in the parent population (bulge) stars, in the interstellar gas that they have expelled, and in subsequent stellar (disk) generations can all be directly observed.

While luminous star formation in disks provides a satisfactory explanation for the ultimate fate of cooled gas in low luminosity ellipticals, it is at present unclear why more luminous, slowly rotating ellipticals do not also have visible stellar disks since cold disks are expected there too (Paper 1). Within the many uncertainties regarding the star formation process, the stellar properties of all elliptical disks can be understood if stars of lower mass are favored in high pressure environments. Maximum interstellar pressures in the most massive ellipticals are about 1000 times that in the interstellar medium of our Galaxy so even the most massive stars formed may not be optically luminous; in low-luminosity ellipticals such as we consider here the pressures are lower so stars at the upper IMF cutoff may be optically luminous but insufficiently massive ($\lesssim 8\ M_{\odot}$) to produce SNII. Alternatively, cold and dynamically fragile stellar disks may have formed in luminous ellipticals and subsequently been destroyed or altered perhaps in the same merging events responsible for the overall boxy shapes of these galaxies. Finally, hot ambient (cluster) gas of low angular momentum may move into luminous ellipticals and greatly reduce the size of cooling flow disks. We hope to address these problems in the near future.

7. ACKNOWLEDGMENTS

We are greatly indebted to Guy Worthey for preparing for us a version of his dial-a-model program that can accommodate younger stars. The referee is thanked for helpful comments and corrections. Our work on the evolution of hot gas in ellipticals is supported by grant NAG 5-3060 of NASA to whom we are very grateful. In addition WGM is partially supported by a UCSC Faculty Research Grant and FB is supported in part by Grant ASI-95-RS-152 from the Agenzia Spaziale Italiana.

References

Arimoto, N., Matsushita, K., Ishimaru, Y., Ohashi, T., & Renzini, A. 1997, (preprint)
Binette, L., Magris, C. G., Stasinska, G., & Bruzual, A. G. 1994, A&A, 292, 13
Binney, J., Davies, R. L., & Illingworth, G.D. 1990, ApJ, 361, 78
Brighenti, F. & Mathews, W. G. 1996, ApJ, 470, 747 (Paper 1)
Brown, T. M., Ferguson, H. C., & Davidsen, A. F. 1994, ApJ, 454, L15
Buson, L. M., Sadler, E. M., Zeilinger, W. W., Bertin, G. Bertola, F., Danziger, J., Dejonghe, H., Saglia, R. P., & de Zeeuw, P. T. 1993, AASup, 280, 409
Ciotti, L., D'Ercole, A., Pellegrini, S., & Renzini, A., 1991, ApJ, 376, 380
D'Ercole, A. & Ciotti, L. 1997, private communication
Davies, R. L., Efstathiou, G., Fall, S. M., Illingworth, G., & Schechter, P. L. 1983, ApJ, 266, 41
Dehnen, W. 1993, MNRAS, 265, 250
de Jong, R. S. & Davies, R. L. 1996,MNRAS (in print)
Dove, J. B. & Shull, J. M., 1994, ApJ, 423, 196
Fabbiano, G., D.-W. Kim, & Trinchieri, G. 1992, ApJS, 80, 531
Faber, S. M., Tremaine, S., Ajhar, E. A., Byun Y-I., Bressler, A., Gebhardt, K., Grillmair, C., Kormendy, J., Lauer, T. R., & Richstone, D. 1997, ApJ, (in press)
Faber, S. M., Trager, S. C., Gonzalez, J. J., & Worthey, G., 1995, in *Stellar Populations*, eds. Gilmore, G., van der Kruit, P. C., Proc. IAU Symp. 164, (Kluwer:Dordreht), 249
Gonzalez, J. J., 1993, Ph.D. thesis, Univ. of California at Santa Cruz
Hernquist, L. 1990, ApJ, 356, 359
Jaffe, W. 1983, MNRAS, 202, 995
Kim, D.-W., Fabbiano, G., & Trinchieri, G. 1992, ApJ, 393, 134
Kormendy, J. & Bender, R. 1996, ApJ, 464, L119
Macchetto, F., Pastoriza, M., Caon, N., Sparks, W. B., Giavalisco, M., Bender, R. & Capaccioli, M. 1996, A&ASup, 120,463
Magris, G., & Bruzual, G. 1993, ApJ, 417, 102
Mathews, W. G. 1989, AJ, 97, 42
Mathews, W. G., 1990, ApJ, 354, 468
Mathews, W. G., 1997, AJ, 113, 755
Nieto, J.-L., Bender, R., Arnaud, J., & Surma, P. 1991, A&A, 244, L25
Phillips, M. M., Jenkins, C. R., Dopita, M. A., Sadler, E. M., & Binette, L. 1986, AJ, 91, 1062
Rix, H.-W., & White, S. 1990, ApJ, 362, 52
Satoh, C. 1980, Publ. Astr. Soc. Japan, 32, 41
Scorza, C. & Bender, R. 1995, A&A, 293, 20
Scorza, C. & Bender, R. 1996, in *New Light on Galaxy Formation*, eds. R. Bender & R. L. Davies (Kluwer:Dordrecht), 55
Turatto, M., Cappellaro, E., & Benetti, S. 1994,AJ, 108, 202
Tremblay, B. & Merritt,D. 1996, AJ, 111, 2243
Tremaine, S., Richstone, D. O., Byun, Y.-I., Dressler, A, Faber, S. M., Grillmair, C., Kormendy, J., & Lauer, T. R. 1994, AJ, 107, 634
Trinchieri, G., & di Serego Alighieri, SD. 1991, AJ, 101, 1647
Tsai, J. C. & Mathews, W. G. 1995, ApJ, 448, 84
van der Marel, R. P. 1991, MNRAS, 253, 710
Worthey G., 1994, ApJS, 95, 107
Worthey, G., Trager, S. C., & Faber, S. M., 1995, in *Fresh Views of Elliptical Galaxies*, eds. Buzzoni, A., Renzini, A., & Serrano, A., ASP Conf. Series 86, 203

Zeilinger, W. W., Pizzella, A., Amico, P., Bertin, G., Bertola, F., Buson, L. M., Danziger, I. J., Dejonghe, H., Sadler, E. M., Saglia, R. P., & de Zeeuw, P. T. 1996 AASup, 120, 257

Table 1. GALACTIC PARAMETERS FOR E0;0[a] GALAXY

Parameter	Value
R_{c*}	63.65 pc
R_e [b]	1.725 kpc
R_t	63.65 kpc
ρ_{*o}	2.373×10^{-19} gm cm^{-3}
M_{*t}	$7.52 \times 10^{10}\ M_\odot$
$\beta = R_{ch}/R_{c*}$	31.623
$\gamma = \rho_{ho}/\rho_{*o}$	6.2448×10^{-5}
M_{ht}	9 M_{*t}
L_B	$1.317 \times 10^{10} L_{B\odot}$
M_B	-19.89
M_V	-20.83
M_{*t}/L_B	5.71
σ_* [c]	291 km s^{-1}

[a]A non-rotating ($k^2 = 0$) E0 galaxy.

[b]Effective radius.

[c]Characteristic velocity dispersion in stellar core, $\sigma_* = (4\pi G \rho_{*o} R_{c*}^2/9)^{1/2}$.

Table 2. GLOBAL COOLING FLOW EVOLUTION

Galaxy	Time (Gyr)	$M_g(hot)$[a] ($10^9 M_\odot$)	$M_g(cold)$[b] ($10^9 M_\odot$)	$L_x(\Delta E)$[c] (10^{39} ergs/s)	R_d[d] (kpc)
E0L;0	4	0.74	3.98	121.8	...
	10	0.59	6.41	34.6	...
	15	0.49	7.38	19.8	...
E0H;0	4	0.76	2.77	72.5	...
	10	0.49	4.17	14.1	...
	15	0.32	4.57	5.10	...
E2L;1	4	0.65	4.03	3.30	∼7.5
	10	0.40	6.47	0.50	∼13.5
	15	0.14	7.55	0.18	∼31.5
E2H;1	4	0.74	2.78	7.48	∼0.75
	10	0.44	4.14	2.37	∼0.75
	15	0.29	4.40	0.13	∼0.65
E6L;1	4	0.53	4.11	1.10	∼27
	10	0.16	6.55	0.16	∼42.5
	15	0.08	7.63	0.053	∼52
E6H;1	4	0.67	2.72	2.34	∼2.3
	10	0.37	4.13	0.20	∼4.5
	15	0.08	4.40	0.017	∼3.8

[a]Total gas mass in the galaxy having temperature $> 10^4$K.

[b]Total gas mass of cooled gas within galaxy with temperature $T = 10^4$K.

[c]Xray luminosity in the ROSAT band.

[d]Disk radius.

Table 3. STELLAR BURSTS IN THE DISK AND BULGE

t_i[a] (Gyr)	E2L;1 $\Delta M(t_i)$[b] ($10^8 M_\odot$)	E2H;1 $\Delta M(t_i)$[b] ($10^8 M_\odot$)
15.0[c]	131.1[c]	131.1[c]
12.5	28.56	27.80
9.5	8.24	9.00
6.5	4.44	4.61
3.5	2.78	2.02
1.7	0.43	0.18
1.1	0.43	0.18
0.4	0.58	0.24

[a]Age of burst.

[b]Mass of burst within $R_e/2$.

[c]Age and mass of galactic bulge within $R_e/2$.

Table 4. Hβ INDICES[a] WITHIN $R_e/2$

	E2L;1	E2H;1
Galaxy alone	1.41	1.41
Disk	2.87	2.29
Galaxy + disk	2.03	1.73

[a]Using Padova evolution tracks.

Figure Captions

Figure 1: Contours of the stellar temperature $\log T_*(R,z)$ (light lines) and azimuthal stellar velocity $v_{*\phi}(R,z)$ (heavy lines) for the E2;1 galaxy. Values of $\log T_*(R,z)$ and $v_{*\phi}(R,z)$ for two contours are labeled (units: K and k s^{-1}); the contours are equally spaced in $\log T_*$ and $v_{*\phi}$.

Figure 2: Variation of the circular velocity $v_{circ}(R)$ (solid lines) and stellar azimuthal velocity $v_{*\phi}(R,0)$ on the equatorial plane in the E2;1 (bold lines) and E6;1 (light lines) galaxies. All velocities in km s^{-1}.

Figure 3: Properties of the E0;0 galaxy (dashed lines) and its interstellar gas after 15 Gyr for two supernova rates: E0L;0 (heavy solid lines) and E0H;0 (light solid lines). a) Variation of stellar density $\rho_*(R)$ and gas density $\rho(R)$ (gm cm^{-3}); b) Variation of stellar temperature $T_*(R)$ and gas temperature $T(R)$ c) Distribution of 0.5 - 4.5 keV X-ray surface brightness $\Sigma_x(R)$ (solid lines) and stellar surface brightness $\Sigma_*(R)$ (dashed line) with projected radius; the vertical normalization is arbitrary.

Figure 4: Plots of the surface density in the disk of cold gas $\Sigma_d(R,t)$ (gm cm^{-2}) as a function of radius R at three times: $t = 4$ Gyr (dot-dashed line), 10 Gyr (dashed line) and 15 Gyr (light solid line) for the a) E2L;1 galaxy, b) E2H;1 galaxy, and c) E6L;1 galaxy.

Figure 5: Equally spaced contours of the logarithm of the ultimate disk radius in parsecs, $\log R_d(R,z)$, for gas ejected from stars throughout the E2L;1 galaxy. Two contours are labeled with values of $\log R_d(R,z)$ in pc.

Figure 6: Four panels describe the interstellar flow in galaxy E2L;1 at time $t_n = 15$ Gyr; all contours are equally spaced. The physical limit of the galaxy is shown with a dashed line. *upper left*: Contours of $\log \rho(R,z)$ with two contours labeled. Velocity arrow at upper left is 50 km s^{-1}; *upper right*: contours of $\log \rho(R,z)$ in the central galaxy with two contours labeled. Velocity arrow at upper left is 50 km s^{-1}; *lower left*: Contours of $\log T(R,z)$ with two labeled; *lower right*: Contours of azimuthal velocity $v_\phi(R,z)$ with two contours labeled in km s^{-1}.

Figure 7: Flow and thermal conditions in the E2H;1 galaxy at $t_n = 15$ Gyr; all contours are equally spaced. The physical limit of the galaxy is shown with a dashed line. *upper panel*: Contours of $\log \rho(R,z)$ with two labeled. Velocity arrow at upper left is 50 km s^{-1}; *lower panel*: Contours of $\log T(R,z)$ with two labeled.

Figure 8: Gas flow in the E6L;1 galaxy at $t_n = 15$ Gyr; all contours are equally spaced. The physical limit of the galaxy is shown with a dashed line. Two contours of $\log \rho(R,z)$ are labeled. Velocity arrow at upper left is 50 km s^{-1}.

Figure 9: X-Ray surface brightness $\Sigma_x(R,z)$ (0.5 - 4.5 keV) distribution in three galaxies after $t = 15$ Gyr viewed perpendicular to the axis of rotation. Two contours are labeled with values of $\log \Sigma_x$ in erg s^{-1} cm^{-2}; all contours are equally spaced. *Top*: $\Sigma_x(R,z)$ for galaxy E2L;1; *middle*: $\Sigma_x(R,z)$ for galaxy E2H;1; *bottom*: $\Sigma_x(R,z)$ for galaxy E6L;1.

Figure 10: Column densities along the disk plane of the E2L;1 galaxy at time $t_n = 15$ Gyr. *Dashed line:* the total vertical column of cooled gas N_{tot}; *solid line:* the maximum column N_i that can be photoionized HII gas. The photoionized column at any radius is $N_{HII} = \min(N_i, N_{tot})$.

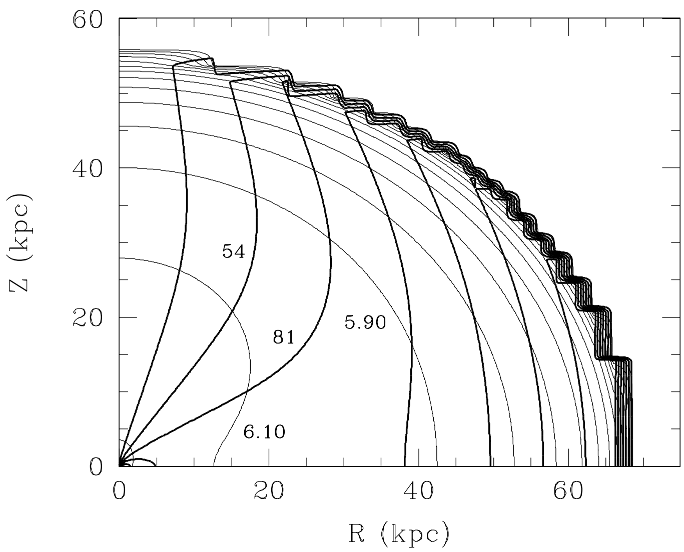

60
40
20
0
Z (kpc)
0
20
40
60
R (kpc)
54
81
5.90
6.10

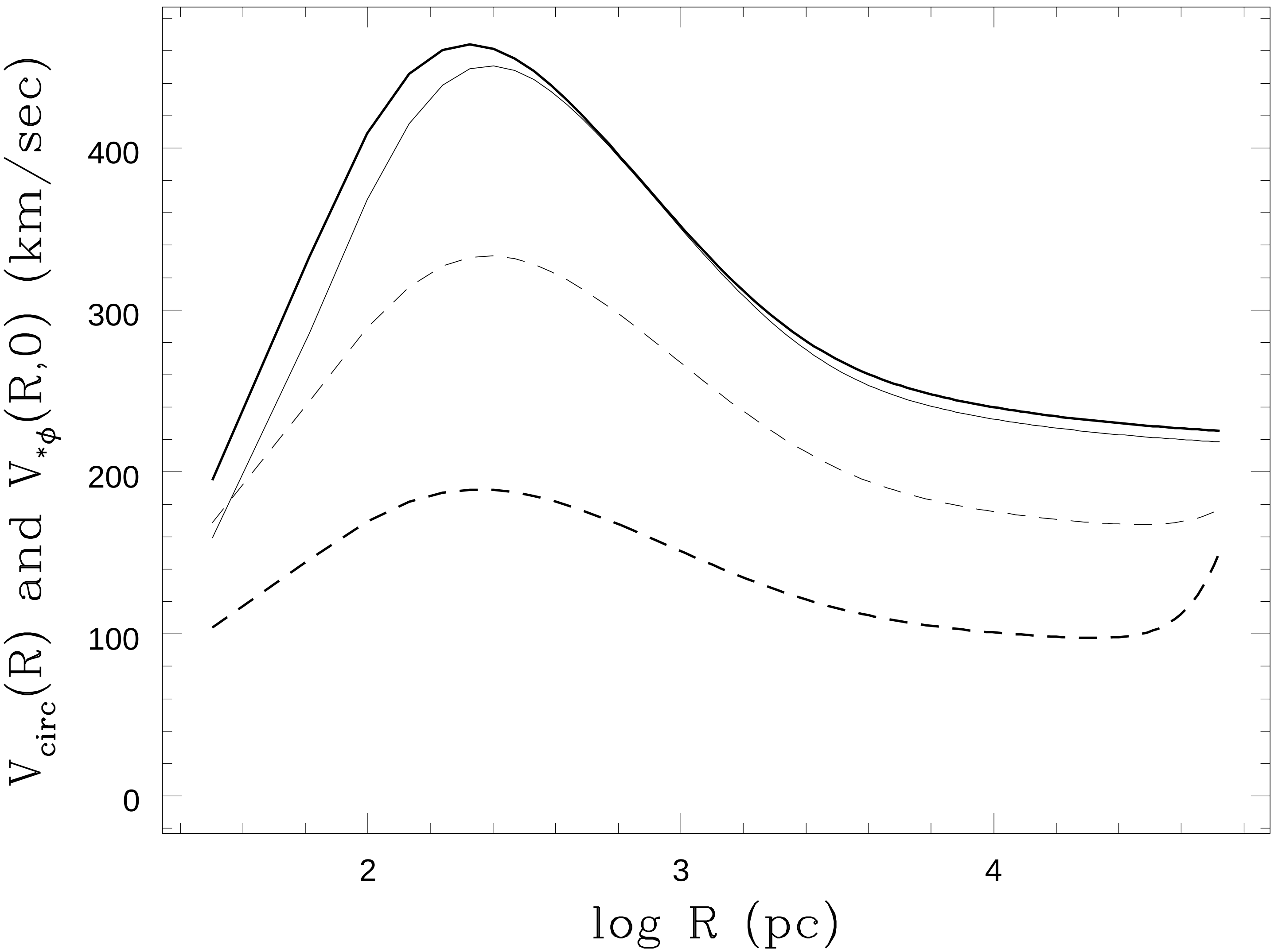

0
100
200
300
400
2
3
4
log R (pc)
V_circ(R) and V_*φ(R,0) (km/sec)

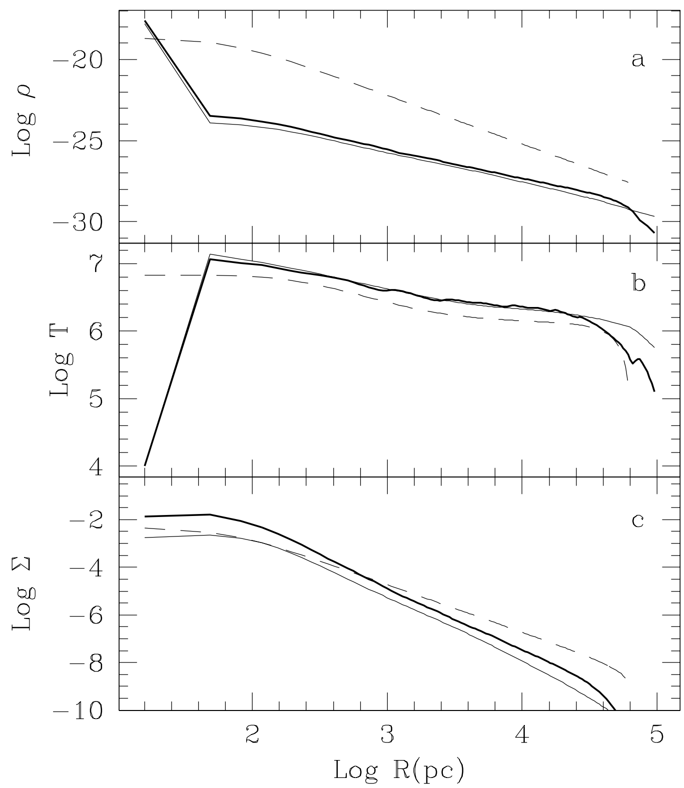

a
b
c
Log ρ
Log T
Log Σ
Log R(pc)
−20
−25
−30
7
6
5
4
−2
−4
−6
−8
−10
2
3
4
5

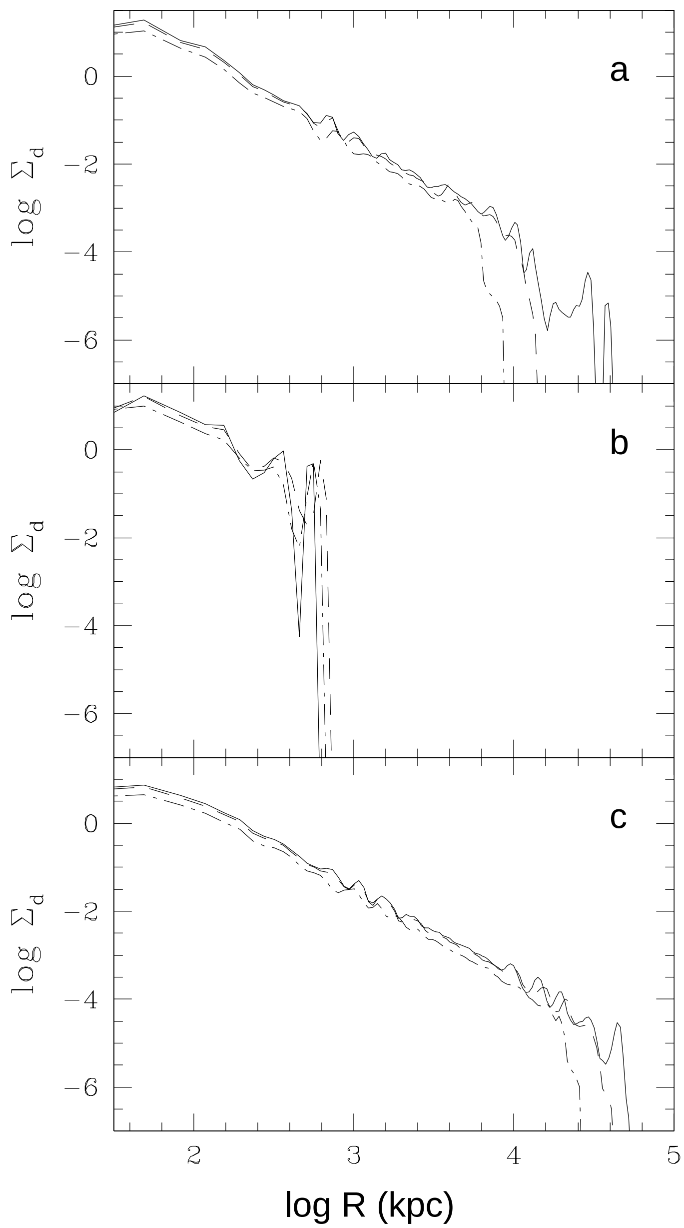
a
b
c
log Σd
0
−2
−4
−6
2
3
4
5
log R (kpc)

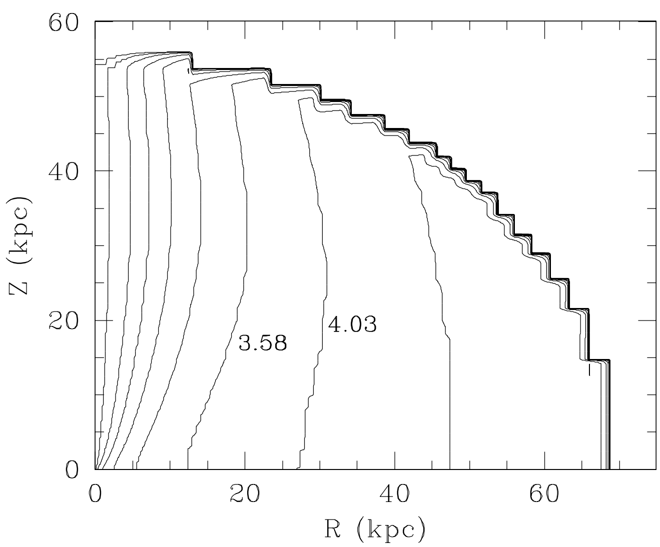
60
40
20
0
Z (kpc)
0
20
40
60
R (kpc)
3.58
4.03

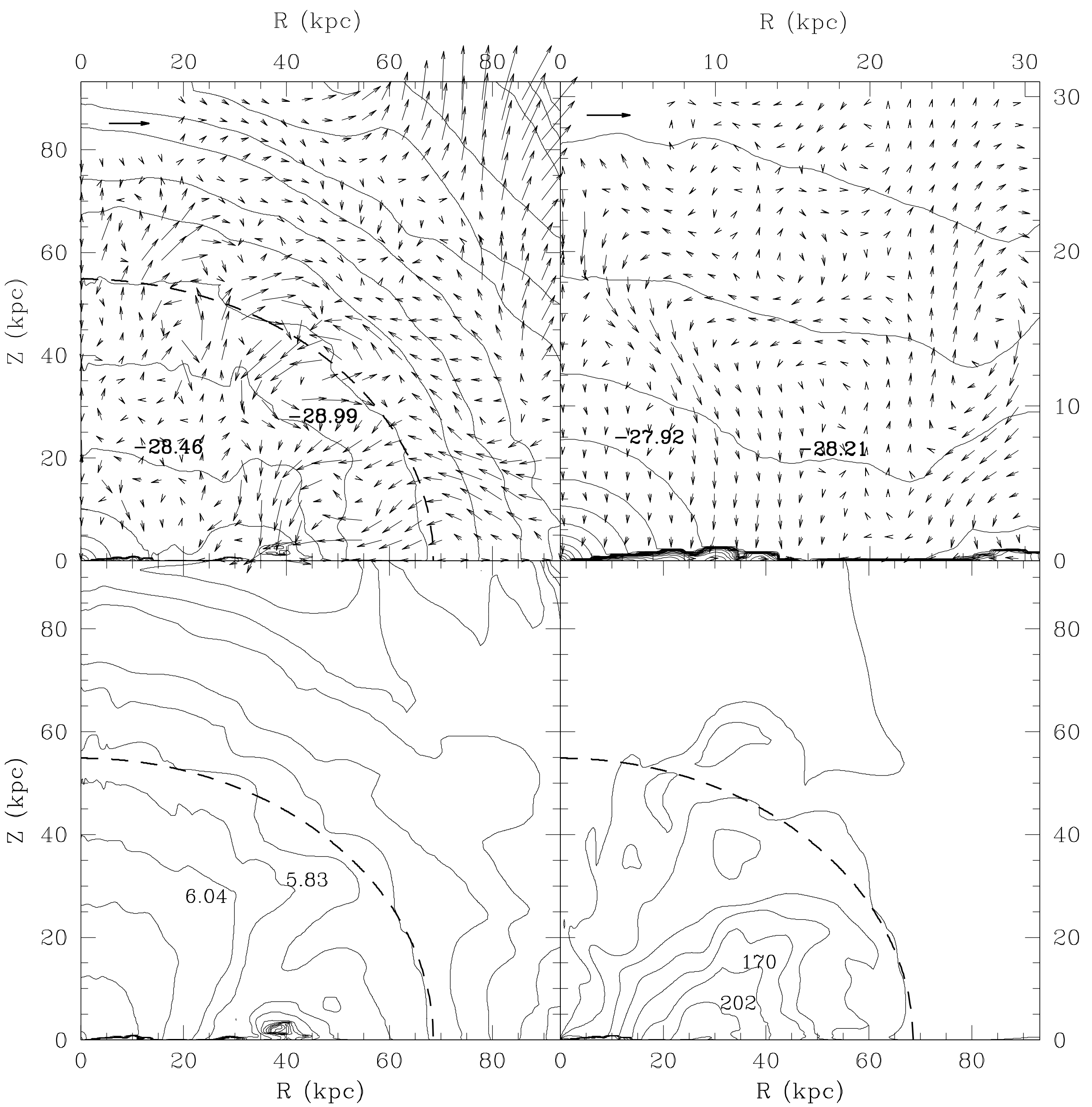

R (kpc)
R (kpc)
Z (kpc)
Z (kpc)
−28.46
−28.99
−27.92
−28.21
6.04
5.83
170
202
R (kpc)
R (kpc)

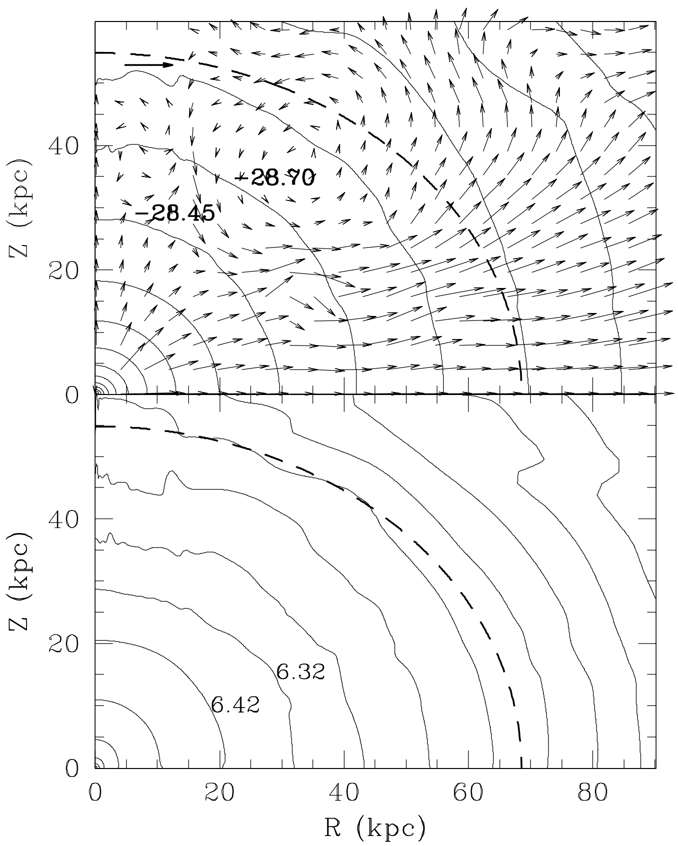

-28.70
-28.45
Z (kpc)
40
20
0
6.32
6.42
Z (kpc)
40
20
0
0
20
40
60
80
R (kpc)

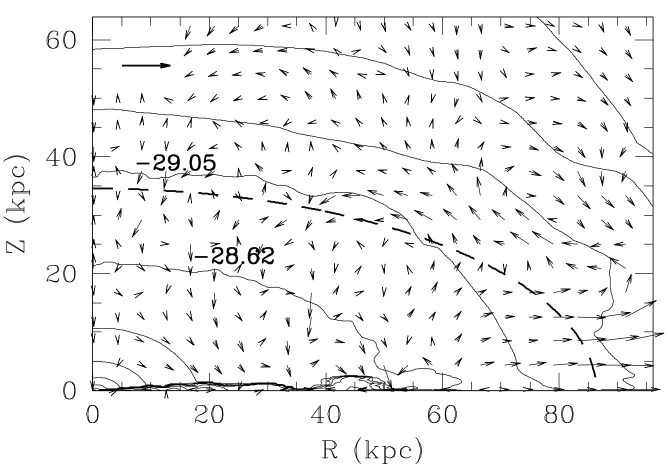

-29.05
-28.62
Z (kpc)
R (kpc)
0
20
40
60
80

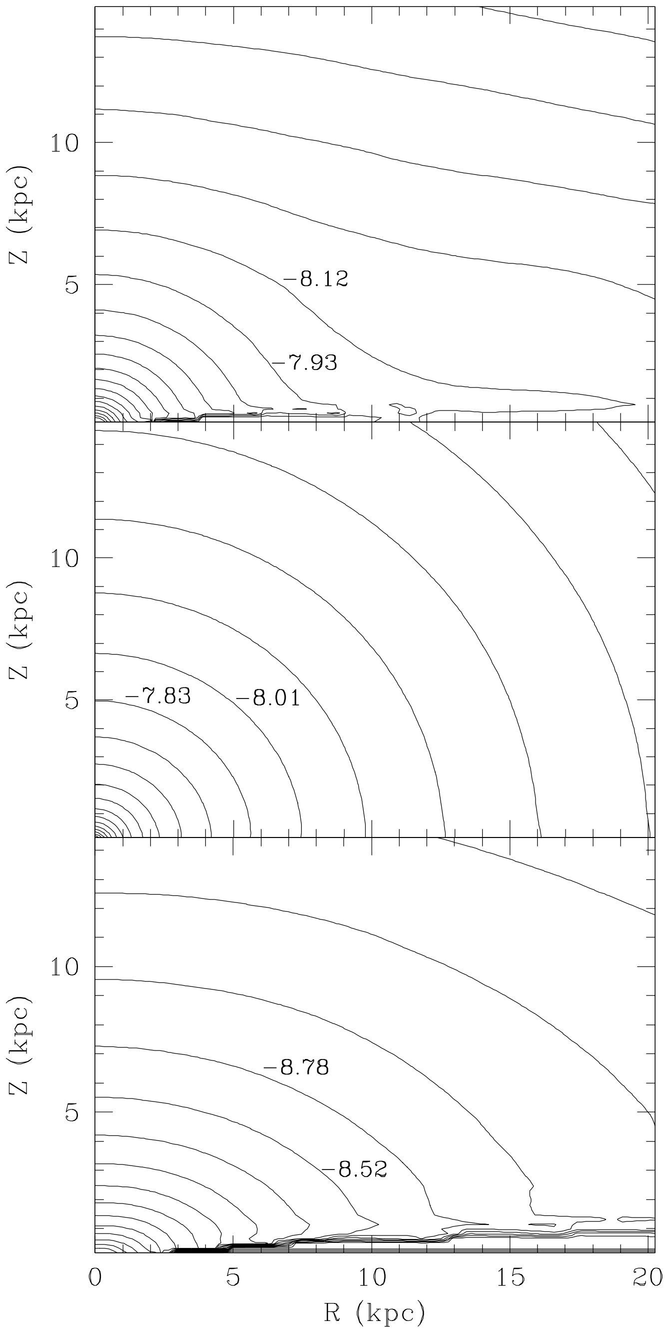

Z (kpc)
10
5
−8.12
−7.93
Z (kpc)
10
5
−7.83
−8.01
Z (kpc)
10
5
−8.78
−8.52
0
5
10
15
20
R (kpc)

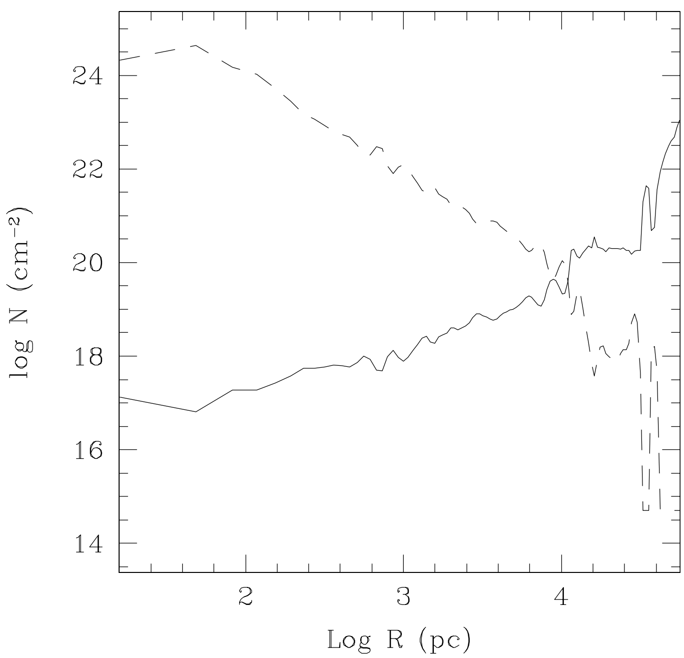

24
22
20
18
16
14
2
3
4
log N (cm⁻²)
Log R (pc)